

# Eco-Friendly Aqueous Dye-Sensitized Solar Cell with a Copper(I/II) Electrolyte System: Efficient Performance under Ambient Light Conditions

Meghry Jilakian and Tarek H. Ghaddar\*

Cite This: *ACS Appl. Energy Mater.* 2022, 5, 257–265

Read Online

ACCESS |



Metrics &amp; More

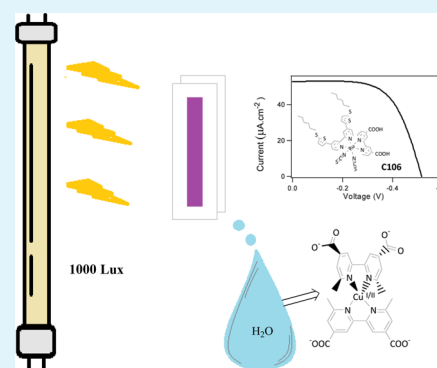


Article Recommendations



Supporting Information

**ABSTRACT:** Organic solvents used in electrolytes of dye-sensitized solar cells (DSCs) are generally toxic and not environmentally safe, which renders their use, especially in indoor solar modules, difficult. In this paper, an eco-friendly DSC is presented based on an aqueous electrolyte system where the redox couple is composed of a water-soluble polypyridyl copper complex,  $[\text{Cu}^{\text{(I)}}(\text{dc-dmbpy})_2\text{Cl}/\text{Cu}^{\text{(II)}}(\text{dc-dmbpy})_2\text{Cl}_2]$ , dc-dmbpy = 6,6'-dimethyl-2,2'-bipyridine-4,4'-dicarboxylate. Good photo-conversion efficiencies (PCE %  $\sim$  7%) have been attained with this water-soluble redox couple under ambient light conditions when coupled with a ruthenium-based dye, C106. This is the first time such a copper complex is in an aqueous DSC and eventually lays a foundation for the further development of eco-friendly water-based DSCs.



**KEYWORDS:** dye-sensitized solar cell, aqueous electrolyte, copper electrolyte, eco-friendly, ambient light

## INTRODUCTION

Since the introduction of the well-known dye-sensitized solar cell (DSC) by O'Regan and Grätzel in 1991,<sup>1</sup> many research groups around the world have been involved until this moment in increasing the DSC efficiency by optimizing dyes' structures, electrolyte systems, counter electrodes, photo-anodes, and so forth. A record power conversion efficiency (PCE %) between 13 and 15% for lab-sized cells has been attained under standard AM1.5G (100  $\text{mW}\cdot\text{cm}^{-2}$ ) solar radiation.<sup>2–5</sup>

For a long time, the iodide/triiodide ( $\text{I}^-/\text{I}_3^-$ ) redox couple has been the conventional electrolyte system for use in DSCs, due to the high efficiencies attained with different types of dye sensitizers especially with the ruthenium-based ones. Despite its remarkable performance in DSCs, scientists have been searching for suitable alternatives due to several reasons. First, the  $\text{I}^-/\text{I}_3^-$  redox couple absorbs light in the visible region, specifically the blue part of the electromagnetic spectrum, and thus lessens the light-harvesting efficiency of the dye-sensitized photo-anode.<sup>6</sup> Furthermore, the reduction of  $\text{I}_3^-$  to  $\text{I}^-$  at the cathode is a two-electron process that causes large internal losses in the cell and high over-potentials that result in lower photo-voltages ( $V_{\text{OC}}$ ).<sup>7</sup> Another drawback of this redox mediator is its corrosiveness when it comes in contact with several metals (especially silver that is used as contact leads), affecting its long-term durability.<sup>8</sup> Two of the best one-electron redox couples that have been demonstrated to outperform the  $\text{I}^-/\text{I}_3^-$  redox couple, especially when coupled with organic-based dyes, are based on cobalt and copper polypyridyl

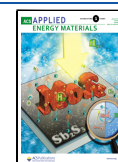
complexes.<sup>9–12</sup> The ease of ligand modification of these complexes makes it possible to control their redox potentials, electron transfer kinetics, and stability, in addition to the tuning of their chemical and physical properties.<sup>13</sup> Hanaya et al. reported one of the highest PCE % (14.3%) that has been obtained with a  $\text{Co}^{\text{(II)}/\text{(III)}}$  electrolyte system and  $V_{\text{OC}}$  values around 1 V,<sup>2</sup> while the highest  $V_{\text{OC}}$  value of 1.24 V has been attained with a  $\text{Cu}^{\text{(I)}/\text{(II)}}$  electrolyte system in acetonitrile by Grätzel et al.<sup>5</sup>

Recently, research in the DSC field has been focused on its indoor use under low-light conditions<sup>14–16</sup> and taking advantage of its aesthetic properties.<sup>17</sup> A recent report by Grätzel et al. reported a record PCE % of 34.5% under ambient light for a co-sensitized solar cell with a  $\text{Cu}^{\text{(I)}/\text{(II)}}$  electrolyte system, attaining a high photo-voltage of 0.98 V at 1000 lux irradiation.<sup>5</sup> Such findings render the use of DSCs to power indoor and low-power electronics very attractive. However, conventional DSCs contain organic solvent-based electrolytes, which have low boiling points and harmful environmental effects. This led our group and other researchers to investigate water-based electrolyte systems in DSCs, which in turn

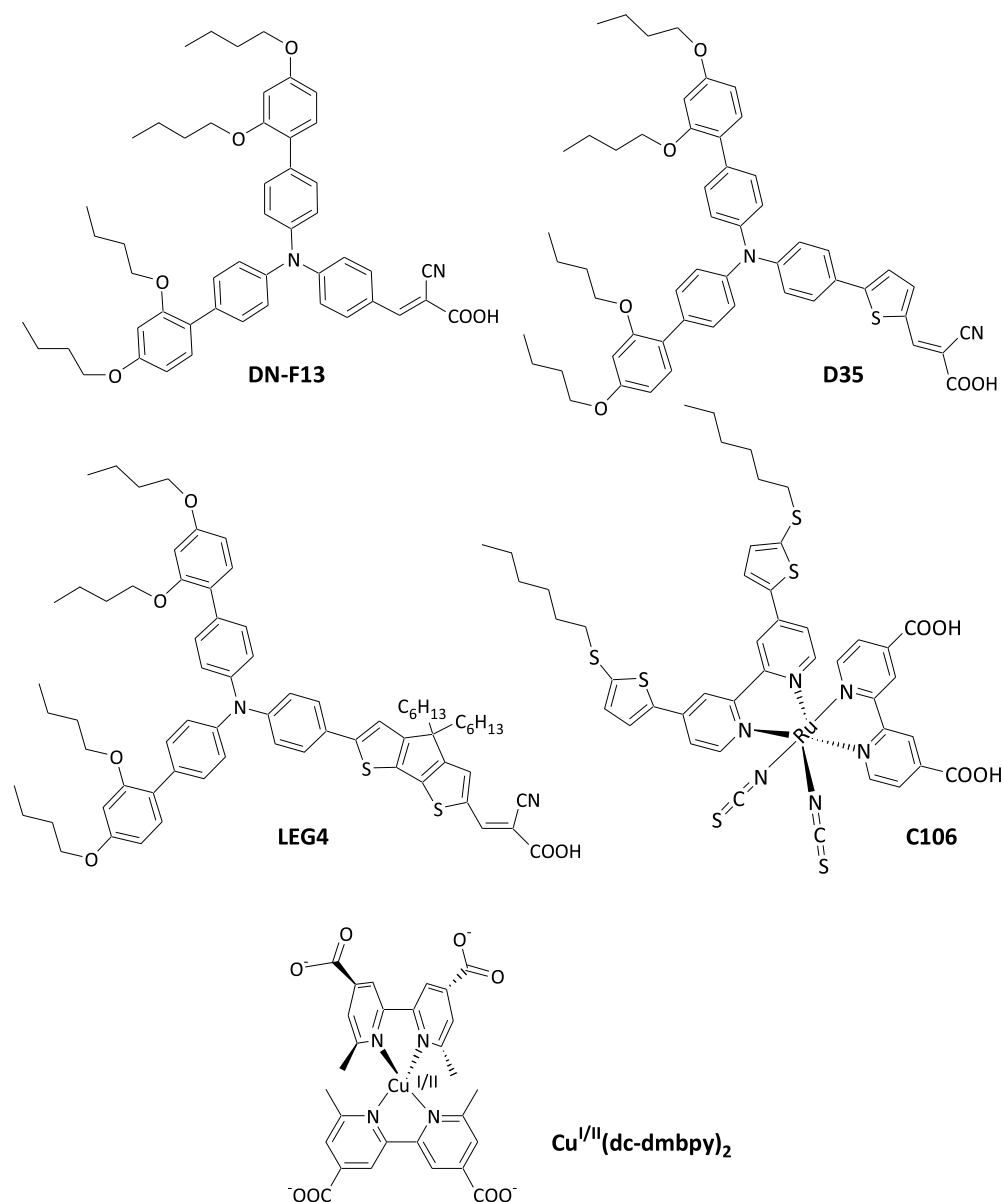
**Received:** September 8, 2021

**Accepted:** January 2, 2022

**Published:** January 11, 2022



**Scheme 1. Molecular Structures of the Copper (I/II) Complex with 6,6'-Dimethyl-2,2'-bipyridine-4,4'-dicarboxylate and the Four Used Dyes in This Study (DN-F13, D35, LEG4, and C106)**



minimizes cost, reduces volatility and flammability, and improves their environmental compatibility.<sup>18–36</sup> Indeed, the most recent reports about this subject have been researching efficiency enhancement and long-term stability of iodide-based aqueous DSCs. DSCs with an aqueous iodide-based redox mediator achieved efficiencies between  $\eta = 2.4$  and 6.0%,<sup>37–39</sup> while most recently, Bella et al. reported a 7% efficient iodide-based aqueous DSC when using a cationic PEDOT counter electrode.<sup>35</sup> Moreover, reports describing the enhancement of the long-term stability of such DSCs with the use of hydrogels such as xanthan gum<sup>36,40</sup> and lignin<sup>41</sup> have also been shown. In addition to the iodide-based aqueous electrolyte systems, other aqueous redox systems have been investigated by different groups such as the thiolate/disulfide redox mediator,<sup>18,25</sup> Fe(CN)<sub>6</sub><sup>4–/3–</sup>,<sup>24</sup> and cobalt(II)/(III) tris(2,2'-bipyridine) redox couple.<sup>29,30</sup> Boschloo and co-workers reported an efficiency of 4.3% in LEG4-sensitized TiO<sub>2</sub> and a water-soluble TEMPO redox couple.<sup>31</sup> Therefore, it becomes

intuitive to investigate new aqueous redox electrolytes and their use in DSCs under ambient light conditions. Eventually, such a research direction would result in commercializing non-toxic and eco-friendly DSCs to power indoor devices such as low-power IoTs.

Herein, we report for the first time on a water-soluble and stable Cu<sup>(I)</sup>(dc-dmbpy)<sub>2</sub>/Cu<sup>(II)</sup>(dc-dmbpy)<sub>2</sub>Cl<sub>2</sub> redox couple, where dc-dmbpy stands for the 6,6'-dimethyl-2,2'-bipyridine-4,4'-dicarboxylate potassium salt and its use in a 100% lewis base-free aqueous DSC sensitized with a ruthenium-based dye, C106,<sup>42</sup> and three organic dyes [LEG4,<sup>43,44</sup> D35,<sup>44,45</sup> and Dyanamo cloudberry orange (DN-F13)],<sup>46</sup> Scheme 1, that shows good performance especially under low-light conditions.

## EXPERIMENTAL SECTION

**Materials and Instrumentation.** All chemicals were purchased from Sigma-Aldrich (Germany) and used as supplied. The C106 dye and titania pastes (18NR-T Transparent and WER2-O Reflector

tania pastes) were purchased from Dyesol (Australia). Fluorine-doped tin oxide (FTO) transparent conducting glasses "Tec 8" and "Tec 15" were purchased from Pilkington (USA). The copper I and II complexes  $\text{Cu}(\text{dc-dmbpy})_2\text{Cl}$  and  $\text{Cu}(\text{dc-dmbpy})_2\text{Cl}_2$  were synthesized using reported methods in the literature.<sup>47</sup>

All of the electrochemical measurements were performed with a CH Instruments 760B potentiostat (USA). The electrochemical setup consisted of a three-electrode cell, with either a gold or FTO working electrode, a Pt wire of 1 mm diameter as the counter electrode, and an Ag/AgCl reference electrode in 0.1 M KCl and  $\text{K}_4\text{Fe}(\text{CN})_6/\text{K}_3\text{Fe}(\text{CN})_6$  as an internal standard (0.57 vs NHE). Electrochemical impedance spectroscopy (EIS) of the DSSCs was performed at  $V_{\text{OC}}$  at different light levels of illumination in the frequency range of 0.1–10<sup>5</sup> Hz with an oscillation potential amplitude of 10 mV at RT. The obtained impedance spectra were fitted with Z-view software (v2.8b, Scribner Associates Inc.).

Photocurrent versus photovoltage characteristics under 1 sun illumination were measured with a Keithley 2400 source meter and a solar simulator illuminated using a 300 W Xenon arc lamp (Oriol) through an AM 1.5 simulation filter (ScienceTech). The irradiated area of the cell was 0.5 × 0.5 cm<sup>2</sup> with a 0.6 × 0.6 cm<sup>2</sup> black mask. For the low-light measurements, a white LED of 13 W (KONNICE, BL13W) was used to irradiate a 1 × 6 cm<sup>2</sup> cell. The average of the photovoltaic parameters of at least three different DSCs is reported. The spectrum and power of the white LED light were measured with a StellarRad spectro-radiometer (Stellar Inc., USA).

The photo-induced absorption (PIA) spectra of the various cells were recorded on a DN-AE02 setup (Dyename, Sweden) over a wavelength range of 500–1000 nm after an (on/off) photo-modulation using a 9 Hz blue LED excitation. White probe light from a tungsten-halogen lamp (20 W) was used as an illumination source. The light was focused onto the sample and then to an automated monochromator (Newport, USA) and detected using a silicon photodiode detector.

**Solar Cell Fabrication.** DSCs were fabricated using standard procedures. Compact  $\text{TiO}_2$  blocking layers were deposited by spray pyrolysis using a hand-held atomizer, following the method developed by Kavan and Grätzel.<sup>48</sup> A solution of 0.2 M titanium di-isopropoxide bis(acetylacetonate) in 2-propanol was sprayed in very short pulses of 1 s duration onto a clean fluorine-doped conductive glass Tec15 placed on a hotplate at 450 °C. This was followed by a pre-treatment process with 40 mM  $\text{TiCl}_4$  aqueous solution at 70 °C for 1 h. A 6 μm mesoporous layer of  $\text{TiO}_2$  was then printed on the glass by the doctor-blading method from a titania paste ( $\text{TiO}_2$  Dyesol 30NR-D), followed by a 6 μm Dyesol WER2-O  $\text{TiO}_2$  paste scattering layer. The electrodes were then sintered at 500 °C for 60 min, followed by a post-treatment process with 40 mM  $\text{TiCl}_4$  aqueous solution at 70 °C for 30 min. Additional heating of the films was carried out at 500 °C for 30 min, cooled to around 80 °C, and then immersed in the dye solution (0.3 mM) in 1:1 *t*-butanol/acetonitrile for 18 h. The PEDOT counter electrodes were prepared by electro-polymerization of the EDOT (3,4-ethylenedioxythiophene) monomer by a periodic reversal potential technique onto the clean conductive glass Tec8. The electrodeposition bath contained an aqueous solution of 0.01 M EDOT and 0.1 M  $\text{LiClO}_4$  with a 24 s pulse at a potential of 1.2 V followed by a 12 s pulse at -0.6 V versus Ag/AgCl. Solar cell assembly was done by sealing the counter electrode to the  $\text{TiO}_2$  working electrode using a 30 μm Surlyn (Dupont) spacer at ~100 °C for 3 min. For long-term stability experiments, cells with dimensions of 1 × 1 cm<sup>2</sup> were assembled while using a 60 μm Surlyn (Dupont) spacer. The electrolyte composed of  $\text{Cu}(\text{I})(\text{dc-dmbpy})_2\text{Cl}$  (0.1 M),  $\text{Cu}(\text{II})(\text{dc-dmbpy})_2\text{Cl}_2$  (0.05 M), 0.1 M KCl, 0.1 M  $\text{LiClO}_4$ , and 0.5% Triton X-100 [in addition to 1% PEG (6000) for large DSCs] in water at pH = 5.6 to 5.8 was introduced through two small holes, previously drilled through the counter electrode, which were then sealed by epoxy glue. The same procedure was applied for the iodide/triiodide electrolyte system that is composed of 2.5 M 1-methyl 3-propyl imidazolium iodide (PMII), 0.05 M iodine, 0.1 M  $\text{LiClO}_4$ , and 0.5% Triton X-100 in water but with a conventional Pt counter electrode. All IV measurements were performed after 3 days from

assembling all the studied DSCs except for the long-term stability tests that started on day 1.

## RESULTS AND DISCUSSION

The copper(I/II) complexes of the 6,6'-dimethyl-2,2'-bipyridine-4,4'-dicarboxylic acid were synthesized using the reported procedure in the literature, where previously, the protonated form as the hexafluoro phosphate salt ( $\text{PF}_6^-$ ) of the Cu(I) complex was used as the first copper-based dye to be incorporated in a DSC.<sup>47</sup> Whereas, in the current study, we took advantage of the water solubility of the same Cu (I) and (II) complexes [ $\sim 0.15$  M for Cu(I) and  $>0.2$  M for Cu(II) as chloride salts] at pHs above 5, and upon optimization, we formulated an aqueous redox couple composed of 0.1 M  $\text{Cu}(\text{I})(\text{dc-dmbpy})_2\text{Cl}$ , 0.05 M  $\text{Cu}(\text{II})(\text{dc-dmbpy})_2\text{Cl}_2$ , 0.1 M KCl, 0.1 M  $\text{LiClO}_4$ , and 0.5% w/w Triton X-100 in water adjusted to a pH between 5.6 and 5.8 with KOH/HCl. The redox potential of the  $\text{Cu}(\text{I})/\text{Cu}(\text{II})$  redox couple in water was determined to be  $E_{1/2} = 0.47$  versus Ag/AgCl ( $E_{1/2} = 0.65$  vs. NHE) by cyclic voltammetry using a gold working electrode. The obtained voltammogram showed a semi-reversible redox reaction for the copper complex in water ( $\Delta E_{\text{pa/pc}} = 85$  mV), Figure 1.

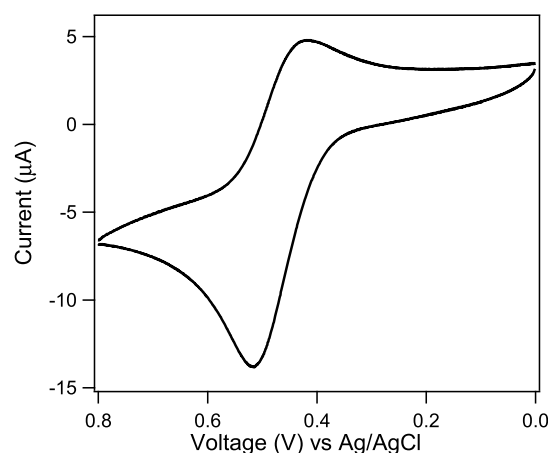


**Figure 1.** Cyclic voltammogram in water (0.1 M KCl) for the  $\text{Cu}(\text{I})/\text{Cu}(\text{II})$  redox couple at a scan rate = 100  $\text{mV}\cdot\text{s}^{-1}$  with a gold working electrode.

The performance of the above-formulated redox couple was assessed by fabricating 100% aqueous-based small (0.5 × 0.5 cm<sup>2</sup>) DSCs with a ruthenium-based dye (C106) and three organic dyes {LEG4, D35, and DN-F13}, (molecular structures of the dyes are shown in Scheme 1). The aforementioned dyes were selected due to their high hydrophobicity, that renders their desorption upon introducing the water-based electrolyte system difficult, and their reported good performance with organic solvent-based electrolyte systems.<sup>42,49,50</sup> The corresponding photo-current versus photo-voltage curves (*I*-*V* curves) measured under standard AM 1.5 G conditions are shown in Figure 2 in addition to a C106-sensitized DSC incorporating an aqueous iodide/triiodide electrolyte system as a reference, and the photovoltaic parameters are summarized in Table 1. Of the three organic dyes, DN-F13 showed the best performance with a  $J_{\text{SC}} = 1.6$   $\text{mA}\cdot\text{cm}^{-2}$ ,  $V_{\text{OC}} = 604$  mV, FF = 0.40, and PCE = 0.39% with the copper-based electrolyte system, while LEG4 and D35 resulted in an overall efficiency PCE = 0.21 and 0.17% ( $J_{\text{SC}} =$

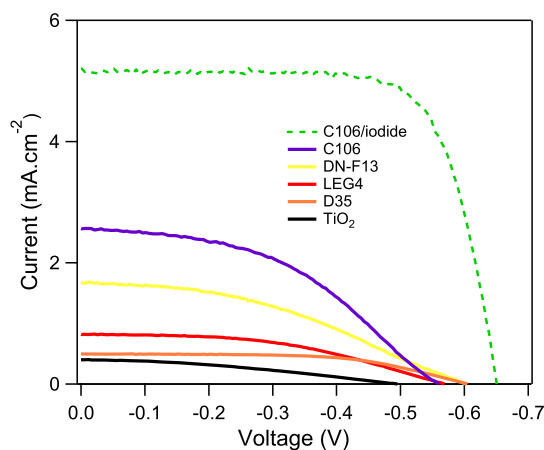


**Figure 2.** Photocurrent–photovoltage response (*IV* curves) of DSCs sensitized with C106 (violet), DN-F13 (yellow), D35 (orange), LEG4 (red), and non-sensitized TiO<sub>2</sub> film (black) with the Cu<sup>(I)</sup>/Cu<sup>(II)</sup> electrolyte system and C106 (dashed-green) with an aqueous iodine/tri-iodide redox system measured under 100 mW·cm<sup>-2</sup>.

**Table 1. Photovoltaic Parameters of the Different DSCs with the Cu<sup>(I)</sup>/Cu<sup>(II)</sup> Electrolyte System and a C106 Reference DSC with an Iodide/Tri-Iodide Aqueous Electrolyte System**

dye	$J_{sc}$ (mA·cm <sup>-2</sup> )	$V_{oc}$ (mV)	FF	PCE (%) <sup>a</sup>
C106 <sup>b</sup>	2.6	559	0.43	0.63
LEG4 <sup>b</sup>	0.8	568	0.46	0.21
D35 <sup>b</sup>	0.5	604	0.56	0.17
DN-F13 <sup>b</sup>	1.6	604	0.40	0.39
TiO <sub>2</sub> <sup>b</sup>	0.4	493	0.35	0.07
C106 with I <sup>-</sup> /I <sub>3</sub> <sup>-c</sup>	5.2	650	0.72	2.44

<sup>a</sup>Measured under a 100 mW·cm<sup>-2</sup> simulated AM 1.5 G spectrum with an active area of 0.5 × 0.5 cm<sup>2</sup> and a black mask (0.6 × 0.6 cm<sup>2</sup>).

<sup>b</sup>Electrolyte: Cu<sup>(I)</sup>(dc-dmbpy)<sub>2</sub>Cl (0.1 M), Cu<sup>(II)</sup>(dc-dmbpy)<sub>2</sub>Cl<sub>2</sub> (0.05 M), KCl (0.1 M), LiClO<sub>4</sub> (0.1 M), and 0.5% Triton X-100 in water at pH = 5.6 to 5.8. <sup>c</sup>Electrolyte: PMII (2.5 M), I<sub>2</sub> (0.05 M), LiClO<sub>4</sub> (0.1 M), and 0.5% Triton X-100 in water.

0.8 and 0.5 mA·cm<sup>-2</sup>,  $V_{OC}$  = 568 and 604 mV, and FF = 0.46 and 0.56), respectively. Surprisingly, the ruthenium-based dye C106 showed the best performance, giving a  $J_{SC}$  = 2.6 mA·cm<sup>-2</sup>,  $V_{OC}$  = 559 mV, and FF = 0.43, with an overall efficiency PCE = 0.63% under the same measurement conditions. Another unexpected result was the DSC device that was not sensitized with any dye, where a small current of  $J_{SC}$  = 0.4 mA·cm<sup>-2</sup> and  $V_{OC}$  = 493 mV (PCE = 0.07%) was seen. We speculate that any Cu<sup>(I)</sup>(dc-dmbpy)<sub>2</sub> from the electrolyte that is adsorbed and/or is weakly bound to TiO<sub>2</sub> can act as a sensitizer and inject electrons upon light irradiation and even get regenerated by the same Cu<sup>(I)</sup> complex in the electrolyte. The latter observation (copper complexes may act as both dyes and mediators) has been demonstrated recently by Roberto et al.<sup>51</sup> The iodide/tri-iodide C106-based reference DSC showed the highest photovoltaic parameters, giving a  $J_{SC}$  = 5.2 mA·cm<sup>-2</sup>, a  $V_{OC}$  = 650 mV, a FF = 0.72, and efficiency PCE = 2.44%.

The incident photon-to-current conversion efficiency (IPCE %) spectra for the sensitized and non-sensitized DSCs are shown in Figure 3. The DN-F13 dye showed a maximum IPCE % value of around 31 to 32% at 430 nm, whereas the onset wavelength of the IPCE % spectrum was 610 nm which is

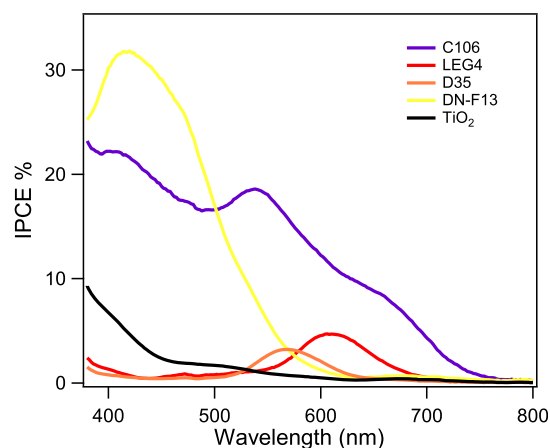


**Figure 3.** IPCE % spectra of DSCs sensitized with the C106 (violet), LEG4 (red), D35 (orange), DN-F13 (yellow) dyes and a non-sensitized titania film (black).

consistent with DN-F13's absorption spectrum. However, D35 and LEG4 demonstrated low IPCE % performance with anomalous behavior at 580 and 607 nm, respectively. Unfortunately, we were not able to assign the exact origin of these two IPCE bands around 600 nm. We hypothesize that this finding might be due to an electron injection from an aggregated form of the dye or an impurity that resembles structurally the parent dye, especially that the band of the LEG4 dye is at a lower energy when compared to that of the D35 one, which is consistent with their band gap energies.<sup>2,44</sup>

In addition, this anomaly is not related to the copper electrolyte system, since the IPCE % spectrum of the non-sensitized titania film in the presence of the copper electrolyte does not show such behavior, but rather a small IPCE % response (1.7% at 480 nm) consistent with TiO<sub>2</sub> sensitization of Cu<sup>(I)</sup>(dc-dmbpy)<sub>2</sub>.<sup>52</sup> Moreover, the IPCE % spectra of LEG4 and D35 suggest very inefficient electron injection from their excited states to the titania conduction band (CB) upon light irradiation, where the latter could be estimated to be around -0.5 V versus NHE at pH = 6.0.<sup>53</sup> At the first site, this value suggests that there should be favoured electron injection reactions from the excited states of D35 and LEG4 since their calculated LUMO ( $E_{ox}^*$ ) are at -0.93 and -0.84 V versus NHE, respectively.<sup>2</sup> However, these  $E_{ox}^*$  values were calculated from  $E_{ox}$  and  $E_{0-0}$  measurements performed in organic solvents and not in water, and therefore, we expect that these values will not hold in our case. However, for the DN-F13 and C106 cases, these are suggested to have a more negative  $E_{ox}^*$  (estimated to be more negative than -1.1 V vs NHE in organic solvents) than D35 and LEG4,<sup>2,44,54,55</sup> and thus show decent electron injection upon photo-excitation. Nevertheless, it was obvious that LEG4 and D35 do not perform well with our aqueous Cu<sup>(I)</sup>/Cu<sup>(II)</sup> electrolyte system, and C106 was selected for further investigation for assessing its regeneration efficiency by the copper electrolyte upon light-induced electron injection.

For this purpose, PIA spectroscopy<sup>56</sup> experiments were performed on C106 DSCs with and without the electrolyte. Figure 4 shows the PIA spectra of nanostructured TiO<sub>2</sub> films sensitized with C106 in the presence and absence of the copper electrolyte, in addition to a reference spectrum of a non-sensitized TiO<sub>2</sub> film in the presence of the copper electrolyte. For the C106-sensitized titania film without the

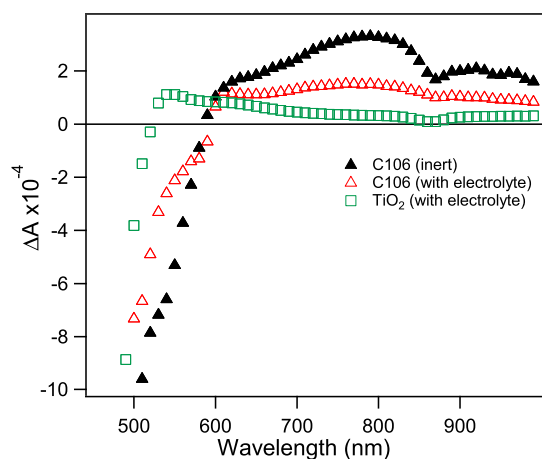


**Figure 4.** PIA spectra of C106-sensitized  $\text{TiO}_2$  films with (red-open triangles) and without (black-solid triangles) the  $\text{Cu}^{\text{I/II}}(\text{dc-dmbpy})_2$  electrolyte, in addition to a non-sensitized  $\text{TiO}_2$  film with the electrolyte (green-open squares).

electrolyte, the spectral characteristics are similar to those found by McGehee et al. for the inert film,<sup>57</sup> where the change in absorption of the oxidized C106 dye species bleaches at 550 nm and has enhanced absorption at 800 nm. However, upon the introduction of the copper electrolyte, there is not a complete disappearance of the positive (>600 nm) and the bleach (<600 nm) signals, which suggests inefficient regeneration of the oxidized C106 dye.

In general, one of the main problems of using 100% aqueous-based electrolyte with hydrophobic dyes, such as the case of C106, is the incomplete wetting of the photoanode by the electrolyte, due to phase segregation, even in the presence of specific surfactants.<sup>19</sup> O'Regan et al. discussed thoroughly in their seminal paper the effect of water on DSCs, where they proved that by reducing the irradiation intensity, the performance mismatch between aqueous and non-aqueous electrolytes decreases. This phenomenon directly arises from the effect of phase segregation of the electrolyte within the titania pores, where empty pores in the photo-anode would result in reduced diffusion of the redox couple within the film, and ultimately affects drastically and negatively the photocurrent.<sup>19</sup> The latter causes a depression in the dye regeneration kinetics at high light intensities, thus suppressing the electron flow in the device and diminishing the short-circuit photocurrent. Figure 5 shows the photocurrent attained by a C106 DSC at different light levels, where again a saturation of the photocurrent is attained at light levels above  $\approx 0.4$  to 0.5 sun, similar to what was seen by O'Regan et al. with a similar hydrophobic dye, TG6,<sup>19,58,59</sup> to the C106 dye in our study. The aforementioned can explain the low  $J_{\text{SC}} = 2.6 \text{ mA}\cdot\text{cm}^{-2}$  of C106 at 1 sun irradiation when compared with values usually attained with organic-based electrolyte systems ( $J_{\text{SC}} > 14 \text{ mA}\cdot\text{cm}^{-2}$ ).<sup>42</sup>

To further evaluate the negative effect of diminished diffusion of the electrolyte species in the film on the C106 DSC performance, EIS measurements were performed at  $V_{\text{OC}}$  under different light intensities.<sup>60–63</sup> Figure 6 shows the Nyquist plots of the C106 DSC incorporating the copper electrolyte system at different applied potentials under light (at  $V_{\text{OC}}$ ). As can be seen, the semi-circle representing the Warburg diffusion becomes more profound at higher light levels compared to the charge transfer resistance at the titania/

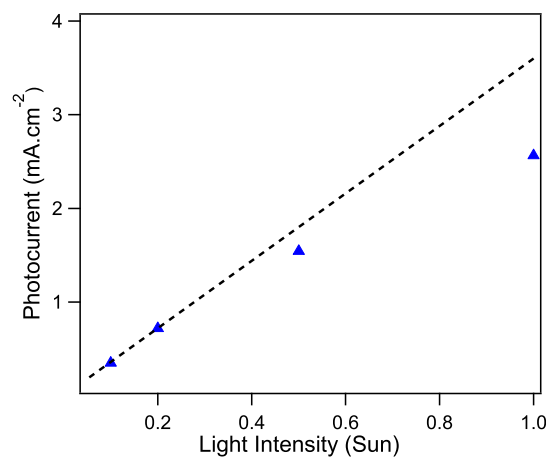


**Figure 5.** Photocurrent ( $J_{\text{sc}}$ ) versus bias light intensity (using a neutral density filter) for a C106 DSC (blue-solid triangles) with the  $\text{Cu}^{\text{I/II}}(\text{dc-dmbpy})_2$  electrolyte.

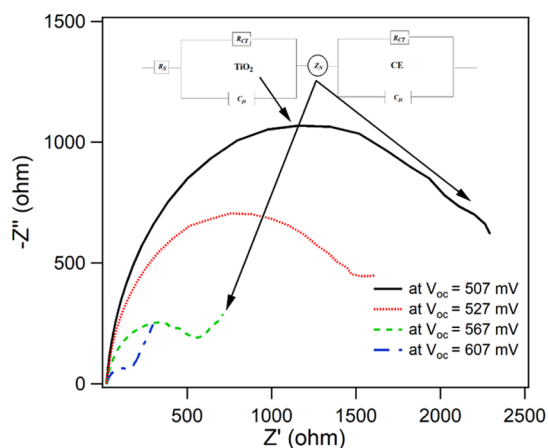


**Figure 6.** Nyquist plots obtained from EIS for the C106 assembled cell with the  $\text{Cu}^{\text{I/II}}(\text{dc-dmbpy})_2$  electrolyte at different applied potentials under light (at  $V_{\text{OC}}$ ).

electrolyte interface. As such, the diffusion impedance would become the limiting factor, thus causing diminished performance at higher light levels. The electron lifetime ( $\tau_n$ ) values derived from the EIS experiments (from EIS  $\tau_n = R_{\text{ct}}C_{\mu}$ ) versus the applied voltage are shown in Figure 7 ( $R_{\text{ct}}$  and  $C_{\mu}$  vs voltage are shown in Supporting Information, Figure S1). Typical  $\tau_n$  values of C106 DSCs with the organic iodide-based electrolyte system prepared in our and other research groups<sup>64</sup> are around 0.1 s at an applied voltage of 0.65 V. However, much lower  $\tau_n \sim 3.5 \text{ ms}$  can be extrapolated from our data at 0.65 V. Again, we speculate that this is due to incomplete regeneration of the oxidized C106 dye by our aqueous electrolyte system and high electron recombination processes between the injected electrons in the titania film and the oxidized form of the C106 dye. Therefore, the insufficient wetting of the  $\text{TiO}_2/\text{C106}$  interface and diminished pore filling by the aqueous electrolyte would lead to the inefficient regeneration of the oxidized dye molecules by the redox species, as suggested also by the PIA spectra (Figure 4).

Following the light intensity dependence results, it becomes intuitive to study the performance of the aqueous-based DSCs under low indoor light intensities, especially since one of the main purposes of using aqueous-based DSCs is the eco-friendliness of such devices. For this purpose, larger ( $6 \times 1$

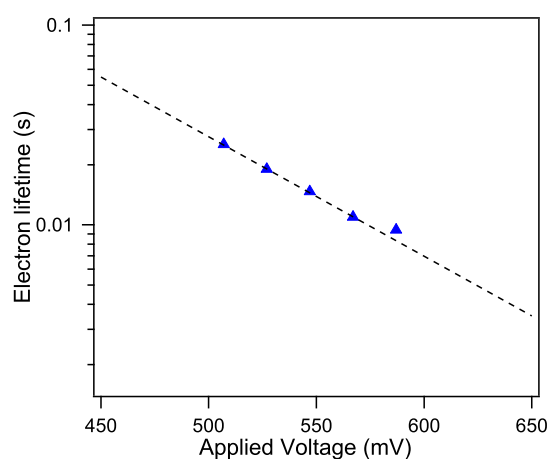


**Figure 7.** Electron lifetimes obtained from EIS of the C106 (blue-solid triangles) assembled cell with the  $\text{Cu}^{\text{I/II}}(\text{dc-dmbpy})_2$  electrolyte.

$\text{cm}^2$ ) C106 and DN-F13 DSCs were assembled with the  $\text{Cu}(\text{dc-dmbpy})_2^{2+/1+}$  redox couple and the performance was studied under light intensities between 100 and 2000 lux using a white LED light source (the LED spectrum is found in Supporting Information, Figure S2). Upon assembling the large ( $6 \times 1 \text{ cm}^2$ ) DSCs, we encountered an incomplete wetting of the photo-anode by the aqueous electrolyte, leaving behind some small areas of the electrode not in contact with the electrolyte. However, this hurdle was circumvented by the addition of 1% w/w of poly-ethylene glycol (PEG, 6000) to the electrolyte system, which led to an immediate and complete visual wetting of the electrode.<sup>26</sup> Interestingly, the 1% PEG additive did not alter the photovoltaic performance of the small-sized DSCs, and accordingly, it was only used for the larger ones. The obtained  $I$ - $V$  curves are shown in Figure 8

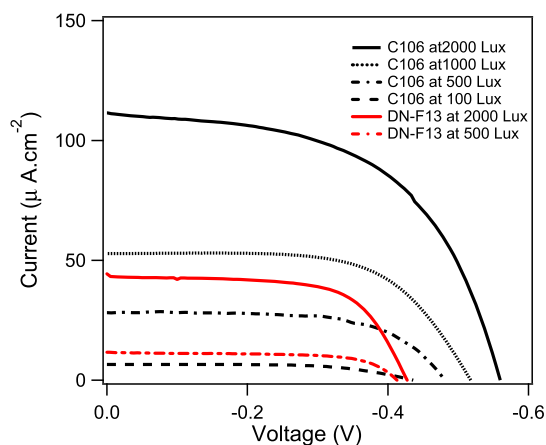


**Figure 8.**  $I$ - $V$  curves of DSCs sensitized with C106 (black) and DN-F13 (red) with the  $\text{Cu}^{\text{I}}/\text{Cu}^{\text{II}}$  electrolyte system measured under 100 (dashed), 500 (dashed-dotted), 1000 (dotted), and 2000 (solid) lux white LED light.

and the photovoltaic parameters are summarized in Table 2. At 100 lux, a  $J_{\text{SC}} = 6 \mu\text{A}\cdot\text{cm}^{-2}$ ,  $V_{\text{OC}} = 433 \text{ mV}$ ,  $\text{FF} = 0.69$ , and an overall efficiency  $\text{PCE} = 7.5\%$  were attained for C106, whereas DN-F13 generated much lower efficiencies at 2000 and 500 lux,  $\text{PCE} = 2.5$  and  $2.4\%$ , respectively. It is worth mentioning here that D35 and LEG4 again showed very low PCEs at the low light levels used, similar to the 1 sun measurements when compared to C106 and DN-F13. As can be seen, the overall

PCE % of C106 ( $\sim 7\%$ ) did not change much at different light levels between 100 and 2000 lux, and hence, these results demonstrate the applicability of using aqueous electrolyte systems in DSCs for indoor operation even at very low light levels, as illustrated by the good PCE % values at 100 lux ( $\sim 0.001$  sun).

In order to test the long-term stability of our aqueous copper-based DSCs, we fabricated two sets of four individual C106 DSCs. The first set was subjected for 30 days to 1 sun light soaking at an open circuit, while the second set was left under ambient light for the same time period. Figure 9 shows the evolution of the average photovoltaic parameters at 2000 lux of both sets versus time. As can be seen, the photovoltaic parameters of both sets show a constant decrease till day 20, after which they stabilize till the end of the long-term stability experiment. Nevertheless, the ambient light and 1 sun soaked DSCs retain more than 60 and 40%, respectively, of the initial PCE % after 30 days, where the latter decrease is majorly due to more profound reduction for the first 20 days in  $J_{\text{SC}}$  and FF versus time. A similar decrease in performance of C106-based DSCs has been seen in our laboratory with water-based electrolytes, especially when it comes to the decrease of  $V_{\text{OC}}$  and FF with time.<sup>18</sup> We attributed this decrease to leaching of the C106 dye into water during the long-term stability test, which we expect to have a similar scenario in this study, but unfortunately, it would be hard to detect any leached C106 by absorption spectroscopy into our highly colored copper-based electrolyte system, as in the previous study.<sup>18</sup> It is worth mentioning here that we also performed a long-term stability test on C106 sensitized cells (four individual cells) incorporating the aqueous iodide/tri-iodide electrolyte system described before under 1 sun illumination for 30 days (see Supporting Information, Figure S3). As can be seen from Figure S3, the PCE % maximizes around 15% at days 5 and 10 from an initial value of PCE % = 11.3% at day 1, while all photovoltaic parameters start decreasing steeply after that, reaching null values by day 30. Upon closely inspecting these cells after day 20, it was obvious that there was profound bleaching of iodine, where by day 30, the electrolyte looked transparent and clear to the naked eye. Therefore, despite the initial good performance of the aqueous iodide/tri-iodide-based electrolyte system with C106, it failed to show long-term stability, which renders its usage in aqueous-based DSCs impractical.

## CONCLUSIONS

In summary, we were successful in formulating a water-soluble and stable redox electrolyte system based on a  $\text{Cu}^{\text{I}}(\text{dc-dmbpy})_2\text{Cl}/\text{Cu}^{\text{II}}(\text{dc-dmbpy})_2\text{Cl}_2$  couple (dc-dmbpy = 6,6'-dimethyl-2,2'-bipyridine-4,4'-dicarboxylate). Even though, and generally speaking, copper-based redox couples in organic solvents perform very well when coupled with organic dyes and not metal-based ones, this was not the case in this study. For small cells under 1 sun irradiation, higher efficiencies of DSCs incorporating a ruthenium-based dye, C106, were attained when compared with the DN-F13 organic dye-based ones ( $\text{PCE} = 0.63$  and  $0.39\%$ , respectively). Interestingly, the most used organic dyes, D35 and LEG4, with copper redox systems in organic media showed very poor performance with photocurrents similar to a non-sensitized DSC. We speculate that the latter two dyes fail to inject electrons upon light irradiation, unlike DN-F13 in an aqueous-based medium, and this is mainly due to the position of the respective dyes'

**Table 2. Photovoltaic Parameters of C106- and DN-F13-Based DSCs with the  $[\text{Cu}(\text{dc-dmbpy})_2]^{2+/1+}$  Electrolyte under Low White LED Light Flux (100 to 2000 lux)**

dye	light intensity (lux)	$J_{sc}$ ( $\mu\text{A}\cdot\text{cm}^{-2}$ )	$V_{oc}$ (mV)	FF	$P_{in}$ ( $\mu\text{W}\cdot\text{cm}^{-2}$ )	$P_{out}$ ( $\mu\text{W}\cdot\text{cm}^{-2}$ )	PCE (%) <sup>a</sup>
C106	2000	110	560	0.55	479.0	33.9	7.1
DN-F13	2000	42	425	0.68	479.0	12.1	2.5
C106	1000	53	518	0.63	238.7	17.2	7.2
C106	500	28	483	0.62	120.1	8.5	7.0
DN-F13	500	10	405	0.72	120.1	2.9	2.4
C106	100	6	433	0.69	24.2	1.8	7.5

<sup>a</sup>Measured under white LED light with an active area  $1 \times 6 \text{ cm}^2$  and a black mask ( $1.2 \times 7.2 \text{ cm}^2$ ). Electrolyte:  $\text{Cu}^{(I)}(\text{dc-dmbpy})_2\text{Cl}$  (0.1 M),  $\text{Cu}^{(II)}(\text{dc-dmbpy})_2\text{Cl}_2$  (0.05 M), KCl (0.1 M),  $\text{LiClO}_4$  (0.1 M), 1% PEG, and 0.5% Triton X-100 in water at pH = 5.6 to 5.8.

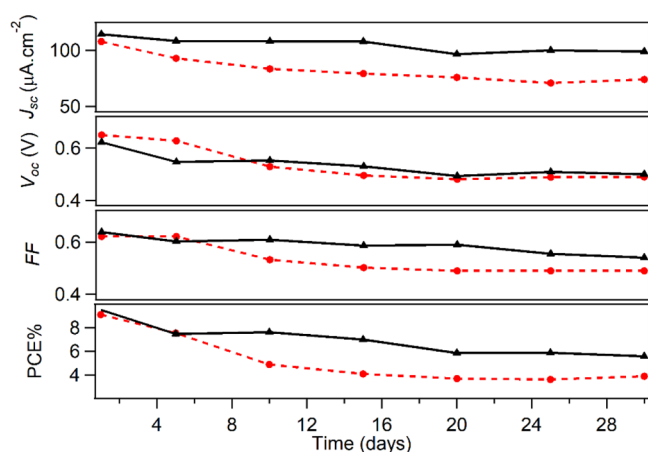


**Figure 9.** Devices' performance at 2000 lux of the aqueous copper-based C106 DSCs soaked under 1 sun (dashed-red) and ambient (solid-black) light at RT for 30 days.

LUMOs and the titania CB. As for the C106-based DSC, light-intensity dependence of photo-currents was seen, where the latter deviates from linearity above 0.4 sun irradiation, which is mainly due to electrolyte diffusion limitation in the pores of the semiconductor upon the phase segregation usually seen in aqueous-based DSCs. Cells sensitized with the C106 dye were successfully tested under low ambient light between 100 and 2000 lux, where the above diffusion limitation is minimized, giving remarkable PCE % values of more than 7%. Finally, our copper-based electrolyte system was tested for its long-term stability when incorporated with the C106 DSCs under 1 sun and ambient light soaking. Under the former conditions, the DSCs retained more than 40% of their initial PCE % at day 30, while the aqueous iodide/tri-iodide analogues deteriorated completely due to iodine bleaching. However, the C106 DSCs retained more than 60% of their initial PCE % values at day 30 when subjected to ambient light. Currently, we are working on an aqueous and quasi-solid version of our copper electrolyte system to further enhance its long-term stability.

## ■ ASSOCIATED CONTENT

### SI Supporting Information

The Supporting Information is available free of charge at <https://pubs.acs.org/doi/10.1021/acsaem.1c02789>.

Further EIS and long-term stability measurements and white LED spectrum (PDF)

## ■ AUTHOR INFORMATION

### Corresponding Author

Tarek H. Ghaddar – Department of Chemistry, American University of Beirut, Beirut 11-0236, Lebanon; [orcid.org/0000-0002-7748-0597](https://orcid.org/0000-0002-7748-0597); Phone: +961-1-350000 (ext. 4057); Email: [tarek.ghaddar@aub.edu.lb](mailto:tarek.ghaddar@aub.edu.lb); Fax: +961-1-365217

### Author

Meghry Jilakian – Department of Chemistry, American University of Beirut, Beirut 11-0236, Lebanon

Complete contact information is available at: <https://pubs.acs.org/10.1021/acsaem.1c02789>

### Notes

The authors declare no competing financial interest.

## ■ ACKNOWLEDGMENTS

This work was supported by the University Research Board (grants 25517 and 26295) at the American University of Beirut (AUB) and the Lebanese National Council for Scientific Research (grant 24350).

## ■ REFERENCES

- O'Regan, B.; Grätzel, M. A low-cost, high-efficiency solar cell based on dye-sensitized colloidal  $\text{TiO}_2$  films. *Nature* **1991**, *353*, 737–740.
- Kakiage, K.; Aoyama, Y.; Yano, T.; Oya, K.; Fujisawa, J.-i.; Hanaya, M. Highly-efficient dye-sensitized solar cells with collaborative sensitization by silyl-anchor and carboxy-anchor dyes. *Chem. Commun.* **2015**, *51*, 15894–15897.
- Yella, A.; Lee, H.-W.; Tsao, H. N.; Yi, C.; Chandiran, A. K.; Nazeeruddin, M. K.; Diau, E. W.-G.; Yeh, C.-Y.; Zakeeruddin, S. M.; Grätzel, M. Porphyrin-Sensitized Solar Cells with Cobalt (II/III)-Based Redox Electrolyte Exceed 12 Percent Efficiency. *Science* **2011**, *334*, 629–634.
- Mathew, S.; Yella, A.; Gao, P.; Humphry-Baker, R.; Curchod, B. F. E.; Ashari-Astani, N.; Tavernelli, I.; Rothlisberger, U.; Nazeeruddin, M. K.; Grätzel, M. Dye-sensitized solar cells with 13% efficiency achieved through the molecular engineering of porphyrin sensitizers. *Nat. Chem.* **2014**, *6*, 242.
- Zhang, D.; Stojanovic, M.; Ren, Y.; Cao, Y.; Eickemeyer, F. T.; Socie, E.; Vlachopoulos, N.; Moser, J.-E.; Zakeeruddin, S. M.; Hagfeldt, A.; Grätzel, M. A molecular photosensitizer achieves a Voc of 1.24 V enabling highly efficient and stable dye-sensitized solar cells with copper(II/I)-based electrolyte. *Nat. Commun.* **2021**, *12*, 1777.
- Tian, H.; Sun, L. Iodine-free redox couples for dye-sensitized solar cells. *J. Mater. Chem.* **2011**, *21*, 10592–10601.
- Rowley, J. G.; Farnum, B. H.; Ardo, S.; Meyer, G. J. Iodide Chemistry in Dye-Sensitized Solar Cells: Making and Breaking I–I Bonds for Solar Energy Conversion. *J. Phys. Chem. Lett.* **2010**, *1*, 3132–3140.

- (8) Wang, M.; Grätzel, C.; Zakeeruddin, S. M.; Grätzel, M. Recent developments in redox electrolytes for dye-sensitized solar cells. *Energy Environ. Sci.* **2012**, *5*, 9394–9405.
- (9) Bai, Y.; Yu, Q.; Cai, N.; Wang, Y.; Zhang, M.; Wang, P. High-efficiency organic dye-sensitized mesoscopic solar cells with a copper redox shuttle. *Chem. Commun.* **2011**, *47*, 4376–4378.
- (10) Sapp, S. A.; Elliott, C. M.; Contado, C.; Caramori, S.; Bignozzi, C. A. Substituted polypyridine complexes of cobalt (II/III) as efficient electron-transfer mediators in dye-sensitized solar cells. *J. Am. Chem. Soc.* **2002**, *124*, 11215–11222.
- (11) Hattori, S.; Wada, Y.; Yanagida, S.; Fukuzumi, S. Blue copper model complexes with distorted tetragonal geometry acting as effective electron-transfer mediators in dye-sensitized solar cells. *J. Am. Chem. Soc.* **2005**, *127*, 9648–9654.
- (12) Zhang, J.; Freitag, M.; Hagfeldt, A.; Boschloo, G. Solid-State Dye-Sensitized Solar Cells. *Molecular Devices for Solar Energy Conversion and Storage*; Springer, 2018; Vol. 1, pp 151–185.
- (13) Stergiopoulos, T.; Falaras, P. Minimizing Energy Losses in Dye-Sensitized Solar Cells Using Coordination Compounds as Alternative Redox Mediators Coupled with Appropriate Organic Dyes. *Adv. Energy Mater.* **2012**, *2*, 616–627.
- (14) Freitag, M.; Teuscher, J.; Saygili, Y.; Zhang, X.; Giordano, F.; Liska, P.; Hua, J.; Zakeeruddin, S. M.; Moser, J.-E.; Grätzel, M.; Hagfeldt, A. Dye-sensitized solar cells for efficient power generation under ambient lighting. *Nat. Photonics* **2017**, *11*, 372.
- (15) Tsai, M.-C.; Wang, C.-L.; Chang, C.-W.; Hsu, C.-W.; Hsiao, Y.-H.; Liu, C.-L.; Wang, C.-C.; Lin, S.-Y.; Lin, C.-Y. A large, ultra-black, efficient and cost-effective dye-sensitized solar module approaching 12% overall efficiency under 1000 lux indoor light. *J. Mater. Chem. A* **2018**, *6*, 1995.
- (16) Saeed, M. A.; Yoo, K.; Kang, H. C.; Shim, J. W.; Lee, J.-J. Recent developments in dye-sensitized photovoltaic cells under ambient illumination. *Dyes Pigm.* **2021**, *194*, 109626.
- (17) Yun, M. J.; Cha, S. I.; Seo, S. H.; Kim, H. S.; Lee, D. Y. Insertion of Dye-Sensitized Solar Cells in Textiles using a Conventional Weaving Process. *Sci. Rep.* **2015**, *5*, 11022.
- (18) Fayad, R.; Shoker, T. A.; Ghaddar, T. H. High photo-currents with a zwitterionic thiocyanate-free dye in aqueous-based dye sensitized solar cells. *Dalton Trans.* **2016**, *45*, 5622–5628.
- (19) Law, C.; Pathirana, S. C.; Li, X.; Anderson, A. Y.; Barnes, P. R. F.; Listorti, A.; Ghaddar, T. H.; O'Regan, B. C. Water-based electrolytes for dye-sensitized solar cells. *Adv. Mater.* **2010**, *22*, 4505–4509.
- (20) Bella, F.; Gerbaldi, C.; Barolo, C.; Grätzel, M. Aqueous dye-sensitized solar cells. *Chem. Soc. Rev.* **2015**, *44*, 3431–3473.
- (21) Murakami, T. N.; Saito, H.; Uegusa, S.; Kawashima, N.; Miyasaka, T. Water-based dye-sensitized solar cells: interfacial activation of TiO<sub>2</sub> mesopores in contact with aqueous electrolyte for efficiency development. *Chem. Lett.* **2003**, *32*, 1154–1155.
- (22) Tikariha, D.; Ghosh, K. K.; Quagliotto, P.; Ghosh, S. Mixed micellization properties of cationic monomeric and gemini surfactants. *J. Chem. Eng. Data* **2010**, *55*, 4162–4167.
- (23) Lai, W. H.; Su, Y. H.; Teoh, L. G.; Hon, M. H. Commercial and natural dyes as photosensitizers for a water-based dye-sensitized solar cell loaded with gold nanoparticles. *J. Photochem. Photobiol., A* **2008**, *195*, 307–313.
- (24) Daeneke, T.; Uemura, Y.; Duffy, N. W.; Mozer, A. J.; Koumura, N.; Bach, U.; Spiccia, L. Aqueous Dye-Sensitized Solar Cell Electrolytes Based on the Ferricyanide–Ferrocyanide Redox Couple. *Adv. Mater.* **2012**, *24*, 1222–1225.
- (25) Tian, H.; Gabrielsson, E.; Lohse, P. W.; Vlachopoulos, N.; Kloo, L.; Hagfeldt, A.; Sun, L. Development of an organic redox couple and organic dyes for aqueous dye-sensitized solar cells. *Energy Environ. Sci.* **2012**, *5*, 9752–9755.
- (26) Xiang, W.; Huang, F.; Cheng, Y.-B.; Bach, U.; Spiccia, L. Aqueous dye-sensitized solar cell electrolytes based on the cobalt(ii)/(iii) tris(bipyridine) redox couple. *Energy Environ. Sci.* **2013**, *6*, 121–127.
- (27) Leandri, V.; Ellis, H.; Gabrielsson, E.; Sun, L.; Boschloo, G.; Hagfeldt, A. An organic hydrophilic dye for water-based dye-sensitized solar cells. *PCCP Phys. Chem. Chem. Phys.* **2014**, *16*, 19964–19971.
- (28) Bella, F.; Gerbaldi, C.; Barolo, C.; Grätzel, M. Aqueous dye-sensitized solar cells. *Chem. Soc. Rev.* **2015**, *44*, 3431–3473.
- (29) Dong, C.; Xiang, W.; Huang, F.; Fu, D.; Huang, W.; Bach, U.; Cheng, Y.-B.; Li, X.; Spiccia, L. Controlling Interfacial Recombination in Aqueous Dye-Sensitized Solar Cells by Octadecyltrichlorosilane Surface Treatment. *Angew. Chem., Int. Ed.* **2014**, *53*, 6933–6937.
- (30) Xiang, W.; Huang, F.; Cheng, Y.-B.; Bach, U.; Spiccia, L. Aqueous dye-sensitized solar cell electrolytes based on the cobalt(II)/(III) tris(bipyridine) redox couple. *Energy Environ. Sci.* **2013**, *6*, 121–127.
- (31) Yang, W.; Söderberg, M.; Eriksson, A. I. K.; Boschloo, G. Efficient aqueous dye-sensitized solar cell electrolytes based on a TEMPO/TEMPO+ redox couple. *RSC Adv.* **2015**, *5*, 26706–26709.
- (32) Vaghiasya, J. V.; Nandakumar, D. K.; Yaoxin, Z.; Tan, S. C. Low toxicity environmentally friendly single component aqueous organic ionic conductors for high efficiency photoelectrochemical solar cells. *J. Mater. Chem. A* **2018**, *6*, 1009–1016.
- (33) Ellis, H.; Jiang, R.; Ye, S.; Hagfeldt, A.; Boschloo, G. Development of high efficiency 100% aqueous cobalt electrolyte dye-sensitized solar cells. *Phys. Chem. Chem. Phys.* **2016**, *18*, 8419–8427.
- (34) Sonigara, K. K.; Vaghiasya, J. V.; Machhi, H. K.; Prasad, J.; Gibaud, A.; Soni, S. S. Anisotropic One-Dimensional Aqueous Polymer Gel Electrolyte for Photoelectrochemical Devices: Improvement in Hydrophobic TiO<sub>2</sub>–Dye/Electrolyte Interface. *ACS Appl. Energy Mater.* **2018**, *1*, 3665–3673.
- (35) Bella, F.; Porcarelli, L.; Mantione, D.; Gerbaldi, C.; Barolo, C.; Grätzel, M.; Mecerreyes, D. A water-based and metal-free dye solar cell exceeding 7% efficiency using a cationic poly(3,4-ethylenedioxythiophene) derivative. *Chem. Sci.* **2020**, *11*, 1485–1493.
- (36) Galliano, S.; Bella, F.; Bonomo, M.; Giordano, F.; Grätzel, M.; Viscardi, G.; Hagfeldt, A.; Gerbaldi, C.; Barolo, C. Xanthan-Based Hydrogel for Stable and Efficient Quasi-Solid Truly Aqueous Dye-Sensitized Solar Cell with Cobalt Mediator. *Sol. RRL* **2021**, *5*, 2000823.
- (37) Law, C.; Moudam, O.; Villarroja-Lidon, S.; O'Regan, B. Managing wetting behavior and collection efficiency in photoelectrochemical devices based on water electrolytes; improvement in efficiency of water/iodide dye sensitized cells to 4%. *J. Mater. Chem.* **2012**, *22*, 23387–23394.
- (38) Law, C.; Pathirana, S. C.; Li, X.; Anderson, A. Y.; Barnes, P. R. F.; Listorti, A.; Ghaddar, T. H.; O'Regan, B. C. Water-Based Electrolytes for Dye-Sensitized Solar Cells. *Adv. Mater.* **2010**, *22*, 4505–4509.
- (39) Choi, H.; Han, J.; Kang, M. S.; Song, K.; Ko, J. Aqueous Electrolytes Based Dye-sensitized Solar Cells using I-/I-3(-) Redox Couple to Achieve ≥ 4% Power Conversion Efficiency. *Bull. Korean Chem. Soc.* **2014**, *35*, 1433–1439.
- (40) Galliano, S.; Bella, F.; Bonomo, M.; Viscardi, G.; Gerbaldi, C.; Boschloo, G.; Barolo, C. Hydrogel Electrolytes Based on Xanthan Gum: Green Route towards Stable Dye-Sensitized Solar Cells. *Nanomaterials* **2020**, *10*, 1585.
- (41) de Haro, J. C.; Tatsi, E.; Fagioliari, L.; Bonomo, M.; Barolo, C.; Turri, S.; Bella, F.; Griffini, G. Lignin-Based Polymer Electrolyte Membranes for Sustainable Aqueous Dye-Sensitized Solar Cells. *ACS Sustainable Chem. Eng.* **2021**, *9*, 8550–8560.
- (42) Cao, Y.; Bai, Y.; Yu, Q.; Cheng, Y.; Liu, S.; Shi, D.; Gao, F.; Wang, P. Dye-Sensitized Solar Cells with a High Absorptivity Ruthenium Sensitizer Featuring a 2-(Hexylthio)thiophene Conjugated Bipyridine. *J. Phys. Chem. C* **2009**, *113*, 6290–6297.
- (43) Tsao, H. N.; Yi, C.; Moehl, T.; Yum, J.-H.; Zakeeruddin, S. M.; Nazeeruddin, M. K.; Grätzel, M. Cyclopentadithiophene Bridged Donor-Acceptor Dyes Achieve High Power Conversion Efficiencies in Dye-Sensitized Solar Cells Based on the tris-Cobalt Bipyridine Redox Couple. *ChemSusChem* **2011**, *4*, 591–594.

(44) Ellis, H.; Eriksson, S. K.; Feldt, S. M.; Gabriellson, E.; Lohse, P. W.; Lindblad, R.; Sun, L.; Rensmo, H.; Boschloo, G.; Hagfeldt, A. Linker Unit Modification of Triphenylamine-Based Organic Dyes for Efficient Cobalt Mediated Dye-Sensitized Solar Cells. *J. Phys. Chem. C* **2013**, *117*, 21029–21036.

(45) Hagberg, D. P.; Jiang, X.; Gabriellson, E.; Linder, M.; Marinado, T.; Brinck, T.; Hagfeldt, A.; Sun, L. Symmetric and unsymmetric donor functionalization. comparing structural and spectral benefits of chromophores for dye-sensitized solar cells. *J. Mater. Chem.* **2009**, *19*, 7232–7238.

(46) Yum, J.-H.; Holcombe, T. W.; Kim, Y.; Yoon, J.; Rakstys, K.; Nazeeruddin, M. K.; Grätzel, M. Towards high-performance DPP-based sensitizers for DSC applications. *Chem. Commun.* **2012**, *48*, 10727–10729.

(47) Constable, E. C.; Redondo, A. H.; Housecroft, C. E.; Neuburger, M.; Schaffner, S. Copper(i) complexes of 6,6'-disubstituted 2,2'-bipyridine dicarboxylic acids: new complexes for incorporation into copper-based dye sensitized solar cells (DSCs). *Dalton Trans.* **2009**, 6634–6644.

(48) Kavan, L.; Grätzel, M. Highly efficient semiconducting TiO<sub>2</sub> photoelectrodes prepared by aerosol pyrolysis. *Electrochim. Acta* **1995**, *40*, 643–652.

(49) Srivishnu, K. S.; Prasanthkumar, S.; Giribabu, L. Cu(ii/i) redox couples: potential alternatives to traditional electrolytes for dye-sensitized solar cells. *Mater. Adv.* **2021**, *2*, 1229–1247.

(50) Li, J.; Yang, X.; Yu, Z.; Gurzadyan, G. G.; Cheng, M.; Zhang, F.; Cong, J.; Wang, W.; Wang, H.; Li, X.; Kloos, L.; Wang, M.; Sun, L. Efficient dye-sensitized solar cells with [copper(6,6'-dimethyl-2,2'-bipyridine)<sub>2</sub>]<sup>2+/1+</sup> redox shuttle. *RSC Adv.* **2017**, *7*, 4611–4615.

(51) Dragonetti, C.; Magni, M.; Colombo, A.; Melchiorre, F.; Biagini, P.; Roberto, D. Coupling of a Copper Dye with a Copper Electrolyte: A Fascinating Springboard for Sustainable Dye-Sensitized Solar Cells. *ACS Appl. Energy Mater.* **2018**, *1*, 751–756.

(52) Büttner, A.; Brauchli, S. Y.; Constable, E. C.; Housecroft, C. E. Effects of Introducing Methoxy Groups into the Ancillary Ligands in Bis(diimine) Copper(I) Dyes for Dye-Sensitized Solar Cells. *Inorganics* **2018**, *6*, 40.

(53) Lyon, L. A.; Hupp, J. T. Energetics of the Nanocrystalline Titanium Dioxide/Aqueous Solution Interface: Approximate Conduction Band Edge Variations between H<sub>0</sub> = -10 and H<sub>-</sub> = +26. *J. Phys. Chem. B* **1999**, *103*, 4623–4628.

(54) Kitamura, T.; Ikeda, M.; Shigaki, K.; Inoue, T.; Anderson, N. A.; Ai, X.; Lian, T.; Yanagida, S. Phenyl-Conjugated Oligoene Sensitizers for TiO<sub>2</sub> Solar Cells. *Chem. Mater.* **2004**, *16*, 1806–1812.

(55) Latini, A.; Panetta, R. Test of Different Sensitizing Dyes in Dye-Sensitized Solar Cells Based on Nb<sub>2</sub>O<sub>5</sub> Photoanodes. *Energies* **2018**, *11*, 975.

(56) Boschloo, G.; Hagfeldt, A. Photoinduced absorption spectroscopy as a tool in the study of dye-sensitized solar cells. *Inorg. Chim. Acta* **2008**, *361*, 729–734.

(57) Hardin, B. E.; Sellinger, A.; Moehl, T.; Humphry-Baker, R.; Moser, J.-E.; Wang, P.; Zakeeruddin, S. M.; Grätzel, M.; McGehee, M. D. Energy and Hole Transfer between Dyes Attached to Titania in Cosensitized Dye-Sensitized Solar Cells. *J. Am. Chem. Soc.* **2011**, *133*, 10662–10667.

(58) Matar, F.; Ghaddar, T. H.; Walley, K.; DosSantos, T.; Durrant, J. R.; O'Regan, B. A new ruthenium polypyridyl dye, TG6, whose performance in dye-sensitized solar cells is surprisingly close to that of N719, the 'dye to beat' for 17 years. *J. Mater. Chem.* **2008**, *18*, 4246–4253.

(59) O'Regan, B. C.; Walley, K.; Juozapavicius, M.; Anderson, A.; Matar, F.; Ghaddar, T.; Zakeeruddin, S. M.; Klein, C.; Durrant, J. R. Structure/Function Relationships in Dyes for Solar Energy Conversion: A Two-Atom Change in Dye Structure and the Mechanism for Its Effect on Cell Voltage. *J. Am. Chem. Soc.* **2009**, *131*, 3541–3548.

(60) Garcia-Belmonte, G.; Boix, P. P.; Bisquert, J.; Sessolo, M.; Bolink, H. J. Simultaneous determination of carrier lifetime and electron density-of-states in P3HT:PCBM organic solar cells under

illumination by impedance spectroscopy. *Sol. Energy Mater. Sol. Cells* **2010**, *94*, 366–375.

(61) Wang, Q.; Ito, S.; Grätzel, M.; Fabregat-Santiago, F.; Mora-Seró, I.; Bisquert, J.; Bessho, T.; Imai, H. Characteristics of High Efficiency Dye-Sensitized Solar Cells. *J. Phys. Chem. B* **2006**, *110*, 25210–25221.

(62) Fabregat-Santiago, F.; Garcia-Belmonte, G.; Mora-Seró, I.; Bisquert, J. Characterization of nanostructured hybrid and organic solar cells by impedance spectroscopy. *Phys. Chem. Chem. Phys.* **2011**, *13*, 9083–9118.

(63) Shoker, T. A.; Ghaddar, T. H. Novel poly-pyridyl ruthenium complexes with bis- and tris-tetrazolate mono-dentate ligands for dye sensitized solar cells. *RSC Adv.* **2014**, *4*, 18336–18340.

(64) Nguyen, L. H.; Mulmudi, H. K.; Sabba, D.; Kulkarni, S. A.; Batabyal, S. K.; Nonomura, K.; Grätzel, M.; Mhaisalkar, S. G. A selective co-sensitization approach to increase photon conversion efficiency and electron lifetime in dye-sensitized solar cells. *Phys. Chem. Chem. Phys.* **2012**, *14*, 16182–16186.

## Recommended by ACS

### Efficient and Thermally Stable Organic Solar Cells via a Fully Halogen-Free Active Blend and Solvent

Huan Zhao, Weijie Song, *et al.*

JANUARY 19, 2023

ACS APPLIED ENERGY MATERIALS

READ 

### Cerium-Doped Indium Oxide as a Top Electrode of Semitransparent Perovskite Solar Cells

Limeng Zhang, Fengzhen Liu, *et al.*

FEBRUARY 20, 2023

ACS APPLIED MATERIALS & INTERFACES

READ 

### Volatile Solvent Additives Enabling High-Efficiency Organic Solar Cells without Thermal Annealing

Hui Lin, Silu Tao, *et al.*

DECEMBER 07, 2022

ACS APPLIED ENERGY MATERIALS

READ 

### Naphthoquinoneoxime-Sensitized Titanium Dioxide Photoanodes: Photoelectrochemical Properties

Niyamat I. Beedri, Sunita Salunke-Gawali, *et al.*

NOVEMBER 03, 2022

ACS OMEGA

READ 

Get More Suggestions >